ION ENGINE NEUTRALIZER EROSION IN LAB AND SPACE

R. A. Kuharski, M. J. Mandell, B. M. Gardner
Science Applications International Corporation

I. Katz, D. Vaughan
Jet Propulsion Laboratory

Abstract

Significant erosion of neutralizer tips has been observed in long-duration chamber tests of the NSTAR and NEXT thrusters. Sources of energetic ions that may cause such erosion include (1) elastic scattering of the high energy ions by the slow moving un-ionized propellant and the background gas; and (2) direct impingement of ions emitted at large angles from the outer edge of the thruster. In this paper we present calculations of neutralizer erosion due to both of these sources, including the difference between lab and space environments, and compare the results with laboratory test data.

Introduction

Large ion thrusters are being developed as propulsion systems for deep space missions. The 30 cm NSTAR thruster, which flew on the DS1 mission, has been subjected to a 30,000 hour extended life test[1] in vacuum chamber conditions. The larger 40 cm NEXT thruster has been exposed to a 2000 hour life test[2]. Both tests showed substantial erosion on the inboard side of the neutralizer. For both the NEXT and NSTAR thrusters, the inboard surface of the neutralizer tube is about 8 cm outside the outer boundary of the grid dish, and the tip is about 9 cm downstream of the bottom of the dish. Thus, ion trajectories originating near the periphery of the dish must make an angle of about 45 degrees relative to the axial direction (or about 30 degrees relative to the outermost beamlet direction for these 15 degree dished grids) in order to strike the neutralizer.

There are two likely sources for energetic ions capable of sputtering neutralizer material. One is elastic scattering of the main beam ions by the slow-moving un-ionized propellant or, under laboratory conditions, by the vacuum chamber background gas. The other is direct impingement of main beam ions emitted at high angles from the outer portion of the thruster.

A careful calculation of the elastic scattering contribution to the neutralizer erosion was performed to see if this would account for the observed erosion. This was done using a

David Vaughan 5/2/05 1:58 PM
Deleted: 23

modified version of the axisymmetric code *PlumeTool*, which is part of the *Electric Propulsion Interactions Code (EPIC)*.[3] The plume source terms (current density and emission angle *vs.* radius) were obtained from experimental measurements of current density and *CEX2D*[4] calculations of beamlet angular distribution. Neutral density was calculated taking into account flow through the ion optics and the observed nonuniformity of neutral density within the discharge chamber. When it became clear that elastic scattering alone was insufficient to explain the observed erosion, the *CEX2D* results were used to calculate the flux of main beam ions to the neutralizer. The combined sputtering rate of both sources is in good agreement with the observed erosion.

In the following, we will outline the calculation methods and show results for the NSTAR (30 cm) thruster. We will then show the corresponding results for the NEXT (40 cm) thruster. Table 1 shows a few relevant properties for the two thrusters. Note that while the NSTAR thruster has a diameter of 30 cm, the diameter of the hole pattern is only 28 cm. For NEXT, a proposal considered in this paper is to mask the outer two centimeters of the thruster, leading to a hole pattern with 36 cm diameter.

Table 1. Some relevant parameters for the NEXT and NSTAR thrusters. (See text for explanation of parenthetic diameters.)

	NSTAR	NEXT
Diameter (cm)	**30 (28)**	**40 (36)**
Beam Energy (eV)	**1100**	**1800**
Current (A)	**1.8**	**3.52**
Mean Current Density (Am^{-2})	**28.8**	**34.1**
Specific Impulse (s)	**3170**	**4100**

Calculation of Main Beam Ion Flux Distribution

Calculation of the ion flux to the neutralizer, whether due to elastic scattering or direct impingement, requires good knowledge of the flux and angular distribution of ions throughout space. In calculating this distribution, one must recognize that each beamlet (*i.e.*, the set of ions emerging from a single accel grid hole) contains its own angular distribution. Thus, to obtain the flux at an external point requires integrating over the surface of the accel grid, taking into account the local current density and angular distribution. The purpose of the calculation described in this section is twofold: (1) to obtain the current of primary ions to the neutralizer and (2 to construct an "equivalent" beam for use in *PlumeTool*.

We used the *CEX2D* code to determine the angular distribution of ions emerging from a beamlet as a function of the beamlet current. Figure 1 shows sample ion trajectories for a high current NSTAR beamlet. Most of the ions are deflected from the symmetry axis by the ion space charge and emerge at angles within ten degrees of the axis. However, the

David Vaughan 5/2/05 1:58 PM
Deleted: 23

outermost few ions cross the axis to emerge at high angles. The largest angle shown in Figure 1 is 18 degrees; by extrapolation the maximum angle for this beamlet is 23 degrees.

By contrast, Figure 2 shows sample trajectories for a low current beamlet. In this case, all the ions cross the symmetry axis, and 90 percent of the ions emerge at angles greater than ten degrees. The highest angle shown in Figure 2 is about 30 degrees; by extrapolation, the maximum angle for this beamlet is about 33 degrees. By calculating numerous trajectory sets for both thrusters, we find that the normalized angular distribution (current per steradian) for a beamlet can be adequately represented by $J_b(\theta) = Ae^{-B\theta}$ for $0.1 < \theta < \theta_{max}$, and $J_b(\theta) =$ constant for $\theta < 0.1$ radian, where the parameters A, B, and θ_{max}, as well as the fraction of current within 0.1 radian, are functions of the beamlet current.

To proceed further, we require measurements of the current density as a function of radial distance from the thruster centerline. Such measurements have been published for both NSTAR[5] and NEXT[6]. However, these measurements require some interpretation because they are taken at four to five centimeters downstream of the engine. The current profiles used in these calculations are based on those measurements and are shown in Figure 3.

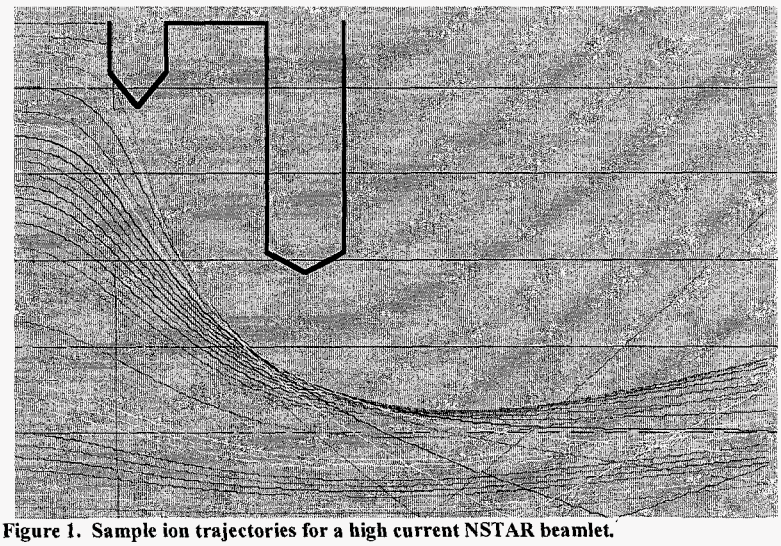

Figure 1. Sample ion trajectories for a high current NSTAR beamlet.

David Vaughan 5/2/05 1:58 PM
Deleted: 23

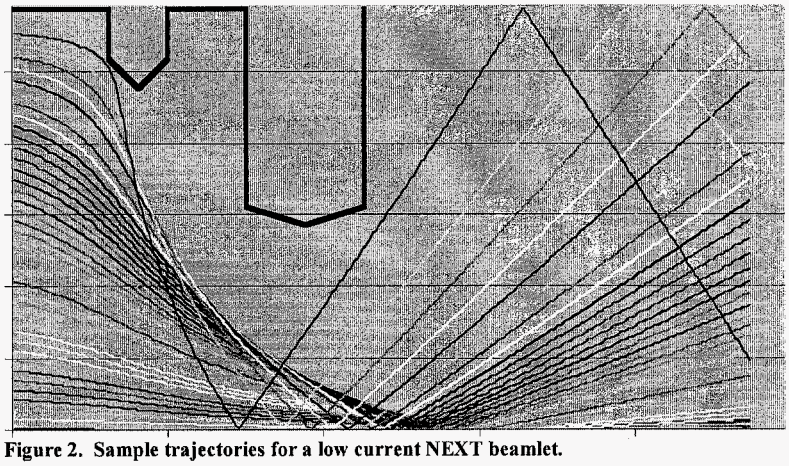

Figure 2. Sample trajectories for a low current NEXT beamlet.

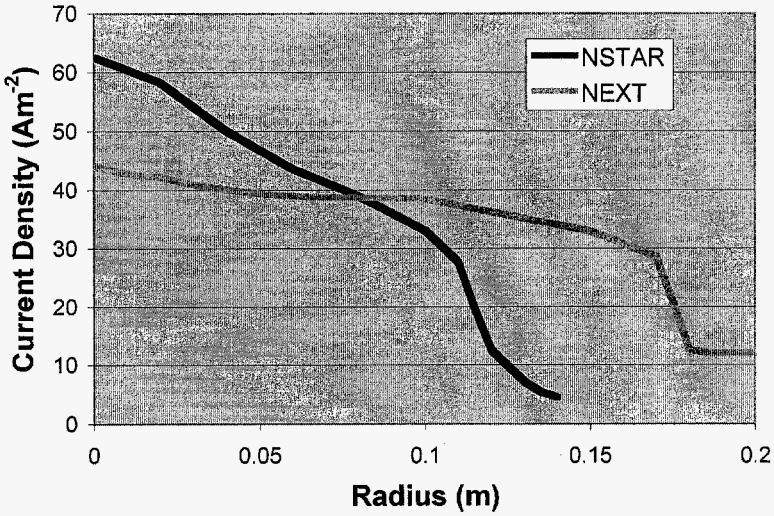

Figure 3. Current density profiles for the NEXT and NSTAR thrusters used in these calculations.

Knowing the current density (hence the beamlet current) and the beamlet current angular distribution, we can calculate the ion flux to a target surface by integrating over the thruster active area:

$$\mathbf{F}(\mathbf{R}) = \int_S d^2\mathbf{r} J(\mathbf{r}) J_b(\mathbf{r},\theta) \frac{(\mathbf{R}-\mathbf{r})}{|\mathbf{R}-\mathbf{r}|^3} \qquad (1)$$

David Vaughan 5/2/05 1:58 PM
Deleted: 23

where **R** is the location of the target surface, J is the accel grid current density, J_b is the normalized beamlet angular distribution appropriate to the beamlet current at **r**, and $\theta = \cos^{-1}(\mathbf{n} \bullet (\mathbf{R} - \mathbf{r})/|\mathbf{R} - \mathbf{r}|)$ with **n** being the normal to the engine surface at **r**. Note that we neglect ion deflection by the beam density gradient electric fields. This is a good approximation due to the high energy of the primary beam ions.

In addition to specifying the current density as a function of radius, it is necessary to specify a set of initial ion angles that increase with radius, in order to generate boundary conditions for *PlumeTool*. To generate this "equivalent plume" we first calculate the ion flux to a distant surface as a function of angle, thereby obtaining the angular distribution of the plume. We then compare the total current within a given radius on the thruster to the current within a given angle on a distant surface, as shown in Figure 4. The angle for each radius is then defined as the angle that contains the same current as the corresponding radius.

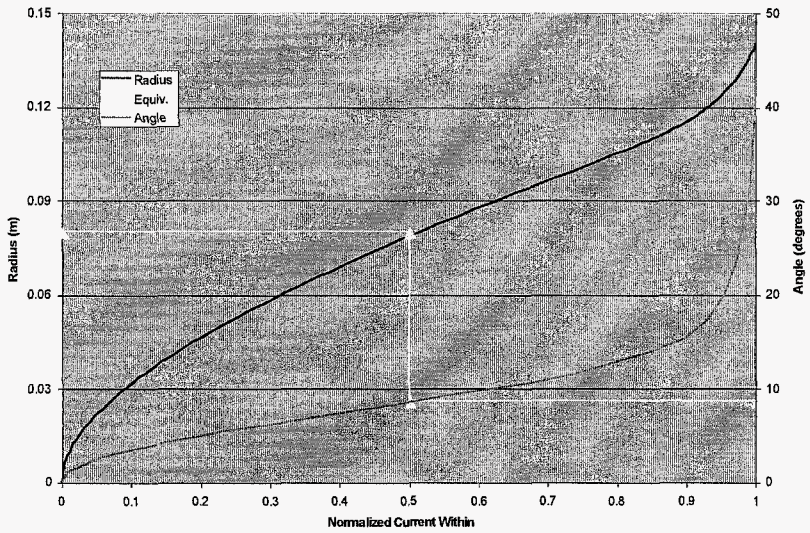

Figure 4. Radius and angle vs. normalized integral current. Yellow lines illustrate scheme by which a radius of 0.08 is assigned an angle of approximately 9 degrees.

PlumeTool propagates the plume from initial current densities and flow angles at the engine exit. The *PlumeTool* initial conditions for NSTAR, calculated as described above, are shown in Figure 5. *PlumeTool* does account for beam expansion due to self-field deflection, leading to very small ion densities at angles greater than indicated in the initial conditions, as shown in Figure 6. Note that in the *PlumeTool* model the high angle ions originate in a very small region at the periphery of the engine, whereas in reality their origins are spread over a few centimeters. However, this result is only being used to

David Vaughan 5/2/05 1:58 PM
Deleted: 23

calculate the elastically scattered ion flux, and the high angle ion currents are too small to make a significant contribution.

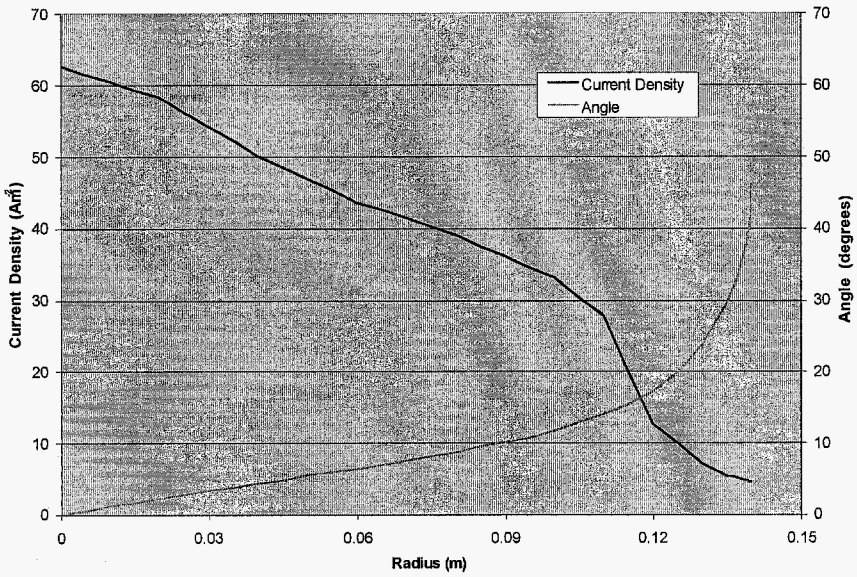

Figure 5. Initial conditions for NSTAR equivalent plume used in *PlumeTool.*

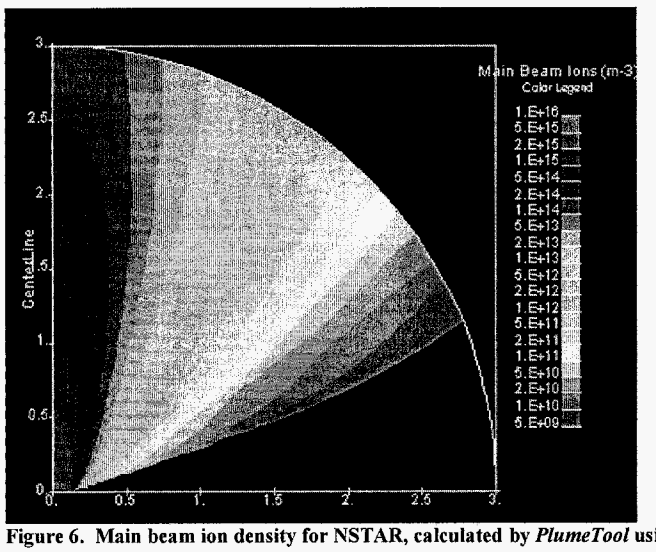

Figure 6. Main beam ion density for NSTAR, calculated by *PlumeTool* using the initial conditions of Figure 5.

David Vaughan 5/2/05 1:58 PM
Deleted: 23

Calculation of Neutral Density

The un-ionized propellant is a highly rarefied gas. The flow of the gas through a hole in either the screen grid or the accelerator grid is an example of the flow of a rarefied gas through a cylindrical channel. This is a well-studied problem. The probability that a gas atom entering the channel will exit the other end is known as the Clausing transmission probability[7] and is a function of the ratio of the length and the radius of the cylinder. The angular distribution of the particles that pass through the cylinder becomes more peaked as the ratio increases. Beijerinck *et al.*[8] derived a formula for the angular distribution of the atoms leaving the cylinder.

The un-ionized gas flow in an ion thruster is not simply the flow through a cylindrical channel, but rather the flow through two cylindrical channels (one in the screen grid and one in the accelerator grid) with a gap between them. We performed a Monte-Carlo simulation to determine how the combination of the two grids would affect the neutral density. The Monte-Carlo calculation for the cylinders is as is described in Beijerinck *et al.*[8]; the space between the grids is treated using hexagonal periodic boundary conditions.

We start simulated atoms at the bottom of the screen grid hole as in a single cylinder simulation[8]. If the atom exits the top of the screen hole it then enters the gap region where we use the periodic boundary conditions to determine its position and velocity when it reaches the accel grid. If the atom enters the hole of the accel grid, it is then traced through the accel grid cylinder using the same algorithm as the screen grid. If it hits the accel grid the atom is re-emitted and traced downward again using periodic boundary conditions to determine its position on reaching the top of the screen. When an atom reaches the top of the screen grid it either enters the hole or is reemitted upward towards the accel grid. Each atom is traced until it either exits from the top of the accelerator grid or the bottom of the screen grid.

We ran a Monte-Carlo simulation with ion-optics parameters appropriate to NSTAR. The screen holes have a length-to-radius ratio of about 0.4, so they do not modify the flow by a large amount. Figure 8 compares the angular distribution of the atoms that exit the top of the accel grid to the angular distribution for a single cylinder with the dimensions of the accel hole. The curves are almost identical, indicating that the presence of the screen grid has very little effect on the angular distribution of the atoms from the accelerator grid. The screen grid will have some tendency to shield the accelerator grid from neutral atoms. From the Monte-Carlo simulation we found that the flux of atoms entering the accel grid was 0.93 times the flux of atoms entering the screen grid. We concluded that we would get an excellent estimate of the density of neutral atoms from a hole in the accel grid by using the angular distribution for cylindrical tube with the same dimensions as the accel grid hole and assuming the density at the accel was decreased to 0.93 of the density at the screen.

David Vaughan 5/2/05 1:58 PM
Deleted: 23

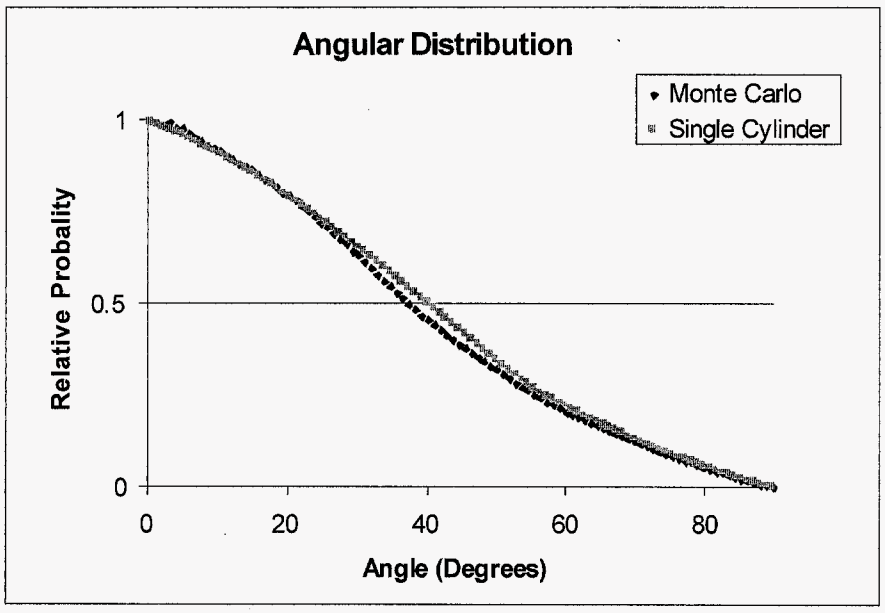

Figure 7. Comparison of angular distribution of neutral effluent for Monte Carlo calculation for screen and accel holes with analytic result for accel hole alone.

The accel grid contains thousands of holes on a dish shaped surface. We modified *PlumeTool* to generate neutral densities at the grid points based on the locations and dimensions of the accel holes, using the treatment described above. The total neutral efflux is determined by taking the propellant flow rate (from the throttle table) and subtracting that portion that is converted to single and double ions.

We account as well for the measured[9] non-uniformity of neutral density in the discharge chamber. The neutral density is depressed near the center of the chamber due to the higher ionization rate, and consequently the neutral efflux is higher for the outer portions of the accel grid, as shown in Figure 8. This is an important effect because, as shown below, most of the sputtering of the neutralizer by elastically scattered ions is due to ions scattered near the outer portion of the thruster.

The resulting neutral density, plotted on the *PlumeTool* computational grid, is shown in Figure 9. For the vacuum chamber case, an additional uniform density of 1.3×10^{17} m^{-3} (corresponding to a pressure of 4×10^{-6} torr at 300K) is added.

David Vaughan 5/2/05 1:58 PM
Deleted: 23

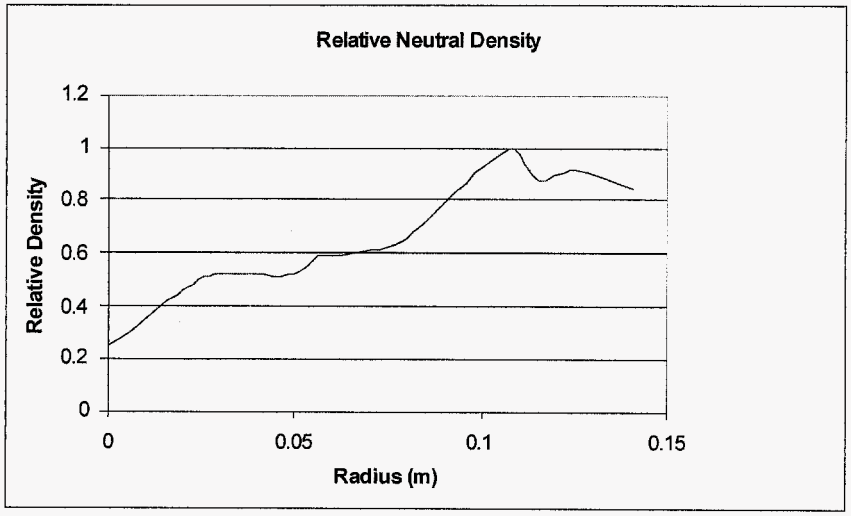

Figure 8. Relative neutral densities in the NSTAR discharge chamber, as measured by Sengupta *et al.*[9]

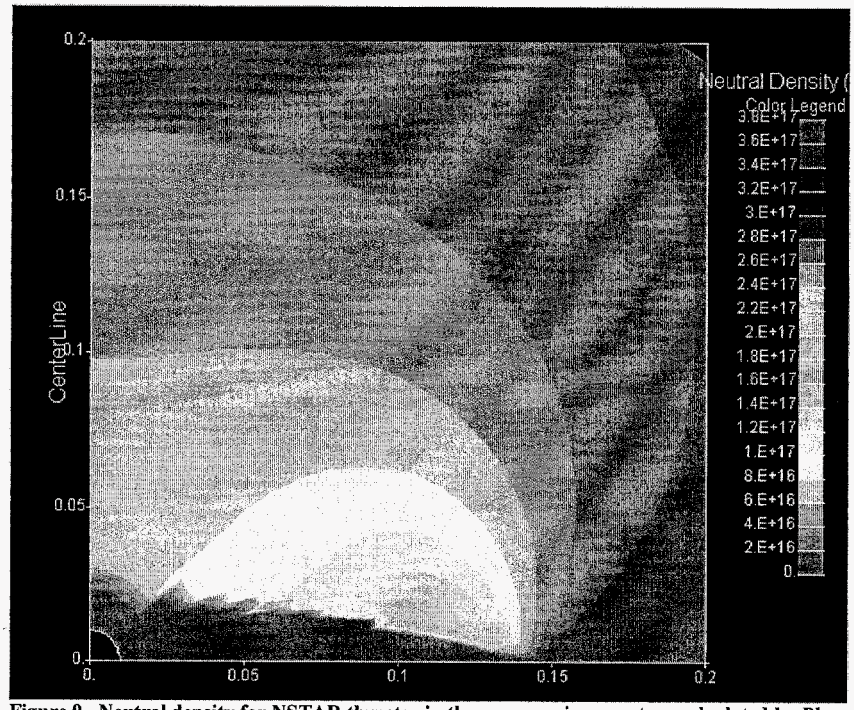

Figure 9. Neutral density for NSTAR thruster in the space environment, as calculated by *PlumeTool*, showing enhanced density near outer portion of thruster.

David Vaughan 5/2/05 1:58 PM
Deleted: 23

Calculation of Sputtering due to Elastic Scattering

Elastic scattering[10,11] of the ion plume by the slow moving un-ionized propellant (and by background gas under laboratory conditions) produces high energy particles at large angles from the thruster axis. *PlumeTool* calculates the elastically scattered ion flux to the neutralizer using the beam flux and neutral density results on its calculation grid. The scattering of the beam by the neutrals to the neutralizer is calculated by rotating each grid element around the thruster axis to form a ring, and then dividing the ring into volume elements. For each such volume element *PlumeTool* calculates the elastically scattered flux seen at the neutralizer using the methods described in reference 11. We multiply by the sputter yield for the appropriate energy and incident angle to obtain that element's contribution to the erosion. The total erosion is determined by summing up the contributions of each element. The accuracy of calculated erosion depends on our determination of the main beam ion flux and neutral density, and our knowledge of the elastic scattering cross-sections and sputter yields.

To calculate the erosion , we need to know the sputtering yield for the Xenon propellant ions incident on the Tantalum neutralizer surface. The sputter yield for normally incident ions is calculated using the formulation of Yamamura and Tawara[12] and is shown in Figure 10.

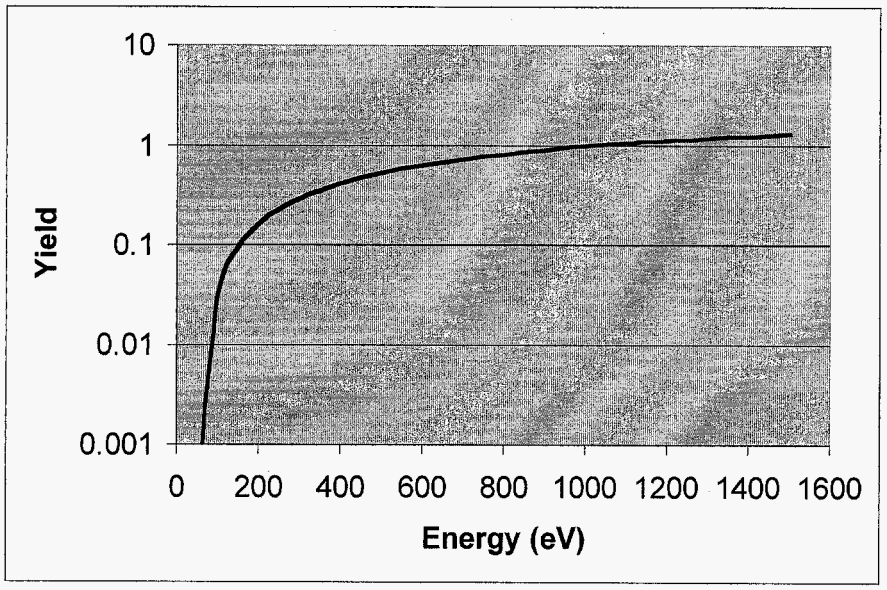

Figure 10. Sputter yield (atoms per ion) for Xenon normally incident on Tantalum, after Yamamura and Tawara, reference 12.

David Vaughan 5/2/05 1:58 PM
Deleted: 23

The sputtering yield also depends on the angle of incidence of the atom to the surface. We adapt the treatment of Yamamura[13] to estimate the yield enhancement due to non-normal incidence, as shown in Figure 11.

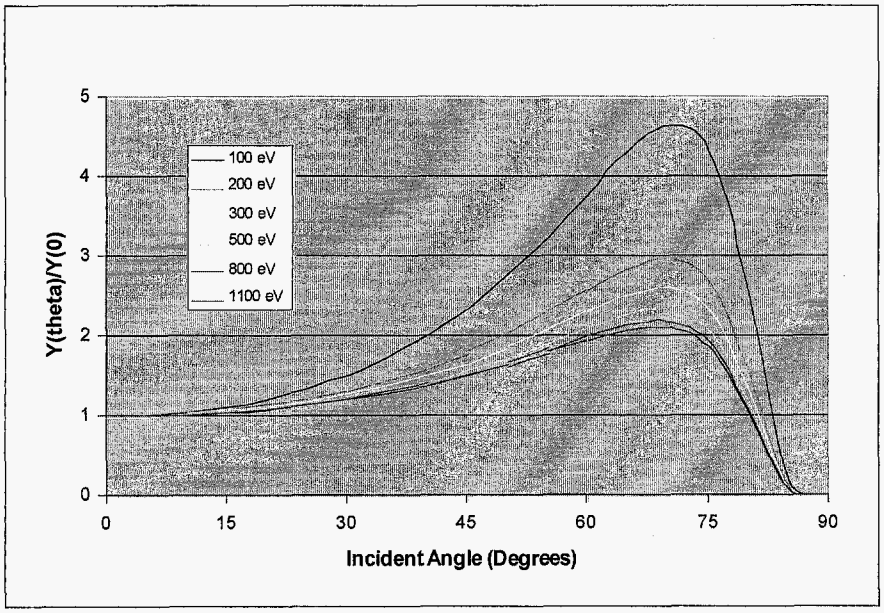

Figure 11. Enhancement of sputter yield for Xenon on Tantalum due to non-normal incidence, adapted from Yamamura, reference 13.

Because of the sensitivity of sputtering rate to incident energy and angle, it is not adequate to estimate erosion due to elastically scattered ions based on the average energy and incident angle. Therefore, *PlumeTool* was modified to perform the erosion calculation internally. For each volume element of the set of rings formed by rotation of the grid elements around the symmetry axis the energy and direction of ions scattered to the neutralizer is well-defined. The sputtering rate was calculated for ions scattered from each such volume element, and summed to obtain the total erosion.

To calculate the sputtering rate correctly several additional factors must be taken into account:

1. The ion beam is about 5.1% doubly ionized. As the double ions have twice the nominal beam energy, they have a higher sputter rate, and must be accounted for separately.
2. From the symmetry of the elastic scattering reaction, a flux of fast neutrals equal to the ion flux is incident on the neutralizer surface. The neutrals are assumed to have the same sputter rate as the ions.

David Vaughan 5/2/05 1:58 PM
Deleted: 23

3. A plasma sheath of about ten volts exists at the neutralizer surface, adding about 10 eV to the energy of the single ions (and about 20 eV to the double ions).

Figure 12 shows the calculated neutralizer erosion due to elastic scattering compared with erosion measurements following the 30,000 hour extended life test. (Measured values were multipled by a factor of 1.38 to normalize to the TH15 throttle condition.) While the results may be in agreement at the lowest point (3 cm below the neutralizer tip), it is apparent that erosion in of the top centimeter of the neutralizer exceeds the calculated erosion by a substantial factor. We will show that this discrepancy is due to direct impingement of high-angle ions from the thruster. However, first we elucidate a few more details of the erosion due to elastic scattering.

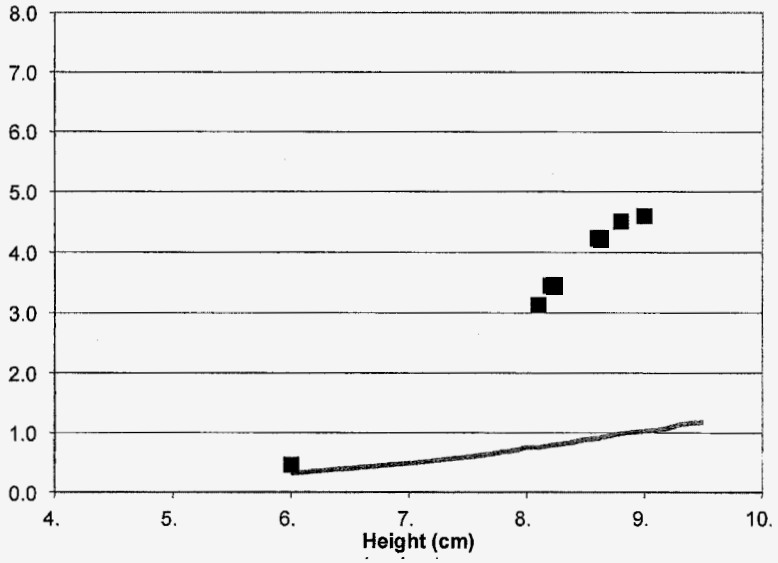

Figure 12. Erosion (microns per 1000 hours) of the NSTAR neutralizer. Curve: Calculated erosion due to elastic scattering under laboratory conditions; Points: Measurement after long-duration ground test, normalized to operation at throttle level TH15.

Sensitivity to neutralizer position

We examined how the sputtering would change if the neutralizer tip position were displaced from the position we had determined. The results are shown in Figure 13. It is apparent that motion of a centimeter in any direction would not significantly change the calculated erosion.

David Vaughan 5/2/05 1:58 PM
Deleted: 23

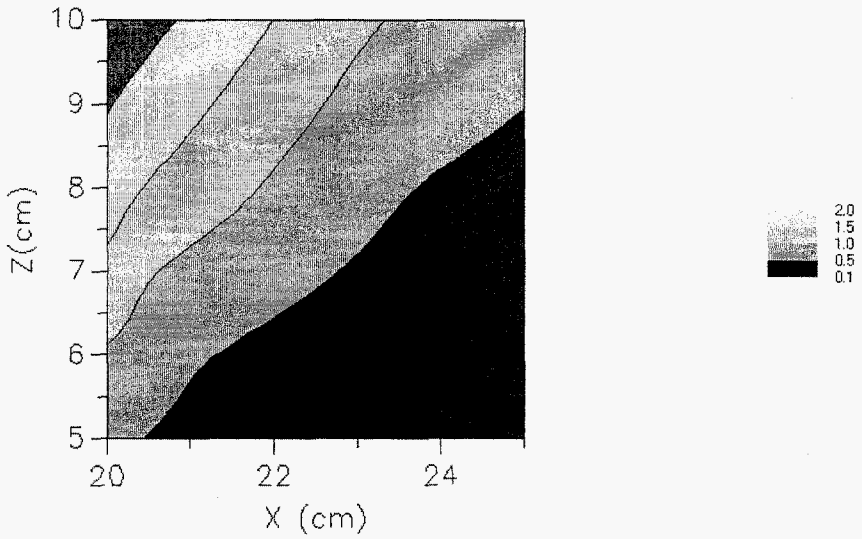

Figure 13. Hypothetical erosion as a function of displaced neutralizer position. The assumed neutralizer tip position is at radial (X) position of 23 cm and axial (Z) position of 9 cm.

Source region for sputtering ions

Figure 14 shows a measure of the amount of erosion due to elastic scattering that occurs in each cell of the *PlumeTool* grid. Most of the collisions that produce the sputtering occur in the vicinity of the accelerator grid at radial values between about 10 and 12 centimeters. Ions scattered to the neutralizer from this region have enough energy to cause sputtering, and the product of beam current and neutral density produces substantial scattered flux. At larger radii, although the scattered ions have higher energy, the flux is much smaller. At smaller radii ions must scatter through a larger angle to reach the neutralizer, and are thus reduced in energy. We believe our knowledge of the beam and neutral density in the source region dominating the erosion is sufficient to give confidence in the calculated results for erosion.

David Vaughan 5/2/05 1:58 PM
Deleted: 23

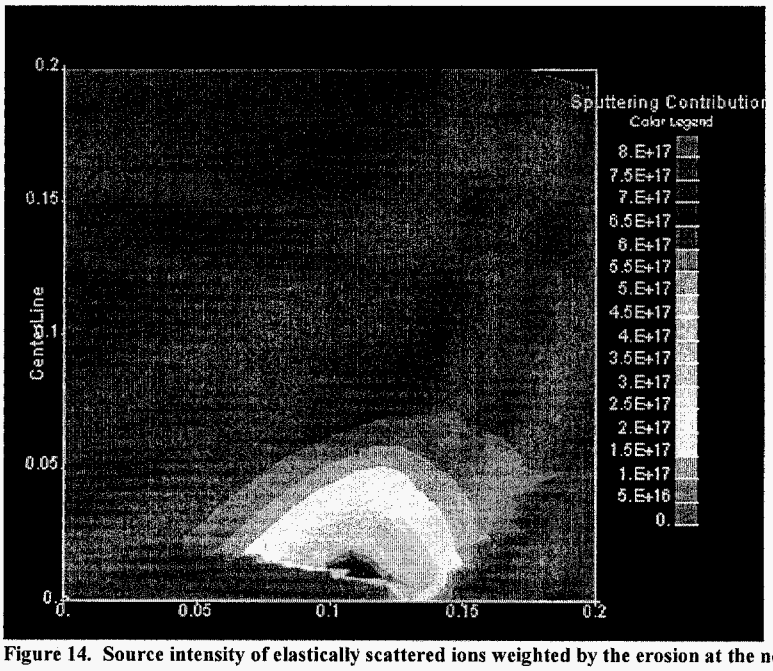

Figure 14. Source intensity of elastically scattered ions weighted by the erosion at the neutralizer tip.

Difference between Lab and Space Conditions

Under laboratory conditions, much of the erosion results from scattering by the background gas in the chamber. We repeated the calculations for the space environment by setting the background gas to 0. Figure 15 shows the calculated values of the erosion for the lab and space environments. The erosion in space is reduced by about 50% from the lab value. This 50% reduction occurs because, in the small region above the thruster where the collisions that lead to sputtering occur, the density of engine neutrals and the density of the chamber background are about equal.

David Vaughan 5/2/05 1:58 PM
Deleted: 23

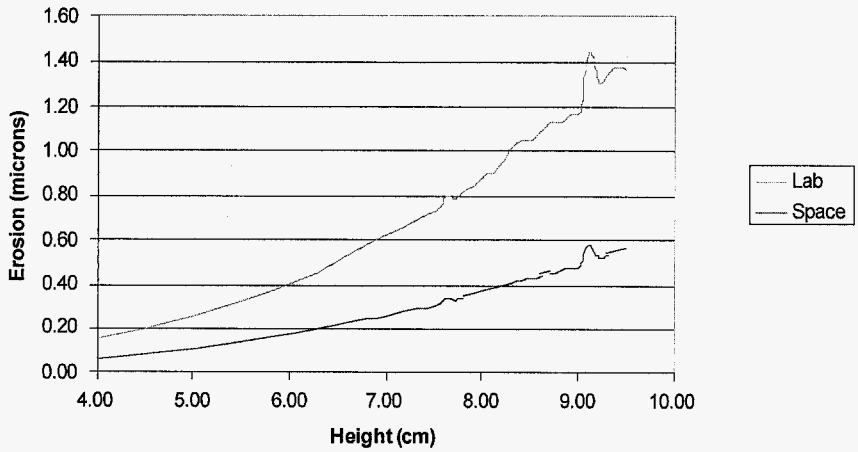

Figure 15. Comparison of erosion along the neutralizer resulting from elastic scattering under laboratory and space conditions.

Calculation of Sputtering due to Direct Impingement

To calculate the direct flux of main beam ions to the neutralizer, we simply apply Equation (1), which calculates the ion flux at a point by integrating over the accel grid surface, to points R on the side of the neutralizer tube facing the thruster's symmetry axis. At the primary beam energy (1100 eV for NSTAR, 1800 eV for NEXT) the normally incident sputter yield is 1.05 for NSTAR and 1.49 for NEXT, and the yield is not overly sensitive to incident angle variation. From geometrical considerations we expect the mean incident angle to be about 45 degrees. For simplicity, we apply a mean sputter yield of 2.0 for NEXT and 1.4 for NSTAR. Figure 16 shows the incident current densities to the inboard side of the neutralizer for NSTAR, NEXT, and NEXT with the outer two centimeters of the accel grid masked. Figure 17 shows the corresponding erosion rates.

Figure 18 shows the calculated erosion of the NSTAR neutralizer compared with what was measured after the 30,000 hour extended life test. Direct impingement dominates the erosion for the upper centimeter of the neutralizer, and the agreement between measurement and calculation including direct impingement is far better than for the calculation for elastic scattering only. The remaining discrepancy is most likely due to the severe erosion and deformation of the accel holes that occurred during the test.

David Vaughan 5/2/05 1:58 PM
Deleted: 23

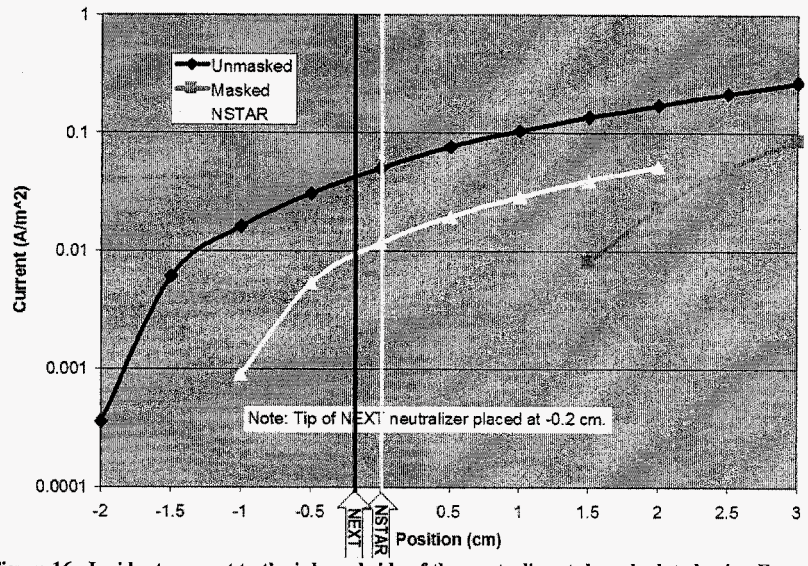

Figure 16. Incident current to the inboard side of the neutralizer tube calculated using Equation 1. Upper (blue) curve is for NEXT, and middle (yellow) curve for NSTAR. Vertical lines indicate the position of the neutralizer tips for the two thrusters. Lowest (magenta) curve is for the NEXT thruster with the outer two centimeters of the accel grid masked.

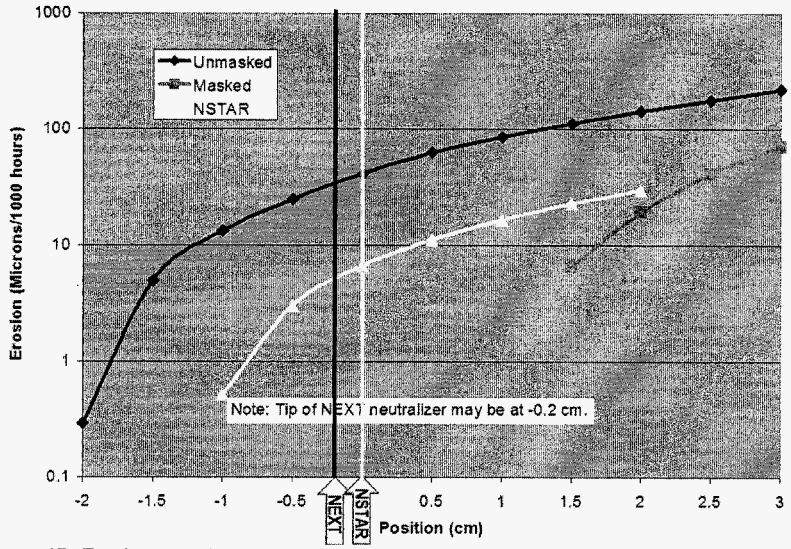

Figure 17. Erosion rates (microns per 1000 hours) corresponding to Figure 16.

David Vaughan 5/2/05 1:58 PM
Deleted: 23

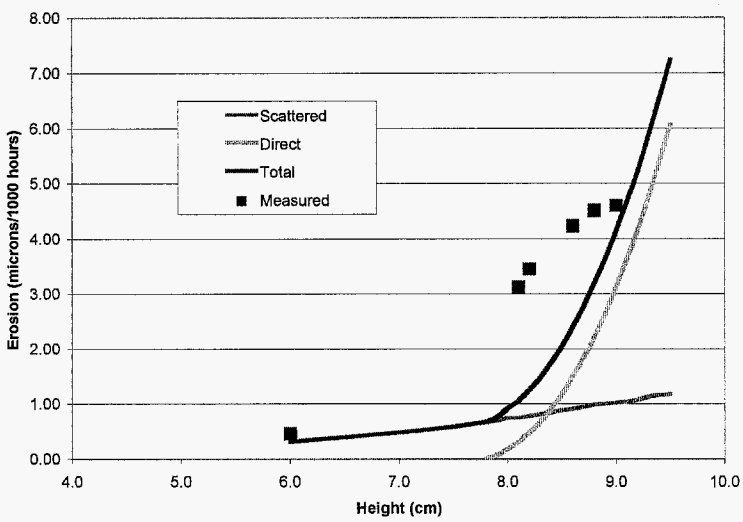

Figure 18. Calculation of erosion of the NSTAR neutralizer, including direct impingement of primary ions, compared with measurement.

Calculations for the NEXT Thruster

Most of the results presented above were for the 30 cm NSTAR thruster. We applied the same techniques to calculate neutralizer erosion for the 40 cm NEXT thruster, using the beam profile, ion optics dimensions, and other parameters appropriate to the larger thruster. We also performed calculations for the larger thruster with the outer two centimeters of the hole pattern masked off. Figures 19-23 show results relevant to the elastic scattering calculation for the NEXT thruster corresponding to those presented previously for NSTAR. The results for direct impingement appear above in Figures 16-17. "Bottom line" results for NEXT appear in Figure 24.

As was the case with the NSTAR thruster, elastic scattering alone cannot explain the magnitude of the observed erosion; direct impingement of primary beam ions is responsible for the bulk of the erosion. The calculated results for NEXT exceed the observed erosion by about 30%, and show about the right profile shape. We consider that this is good agreement, and validates our computational model.

When the outer two centimeters of the NEXT accel grid are masked there is no direct impingement to the neutralizer, and of the only erosion is that due to elastically scattered particles. The reason for this is not that the maximum beam angle is very much reduced, but because ions that originate within 18 cm of the symmetry axis miss the neutralizer, even when emitted at the maximum angle.

David Vaughan 5/2/05 1:58 PM
Deleted: 23

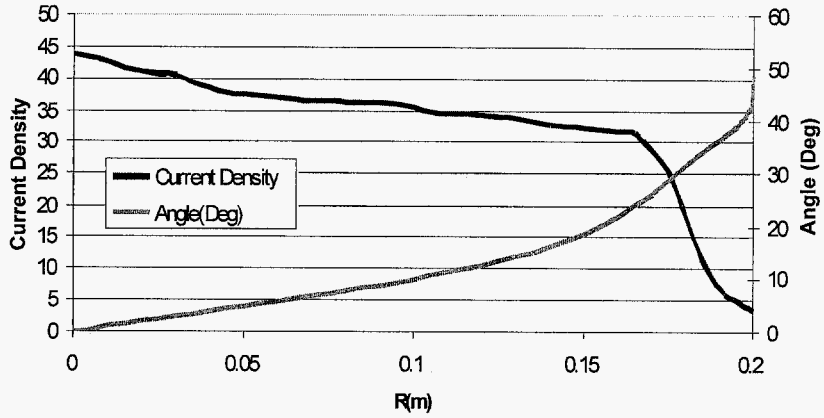

Figure 19. Current density profile and initial angles used as initial conditions for the NEXT calculations.

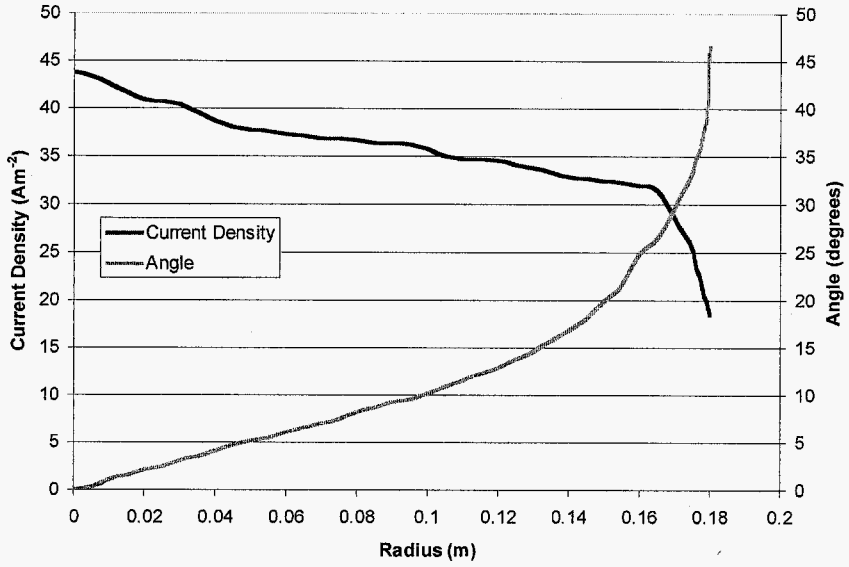

Figure 20. Current density profile and initial angles used as initial conditions for the masked version of the NEXT calculations.

David Vaughan 5/2/05 1:58 PM
Deleted: 23

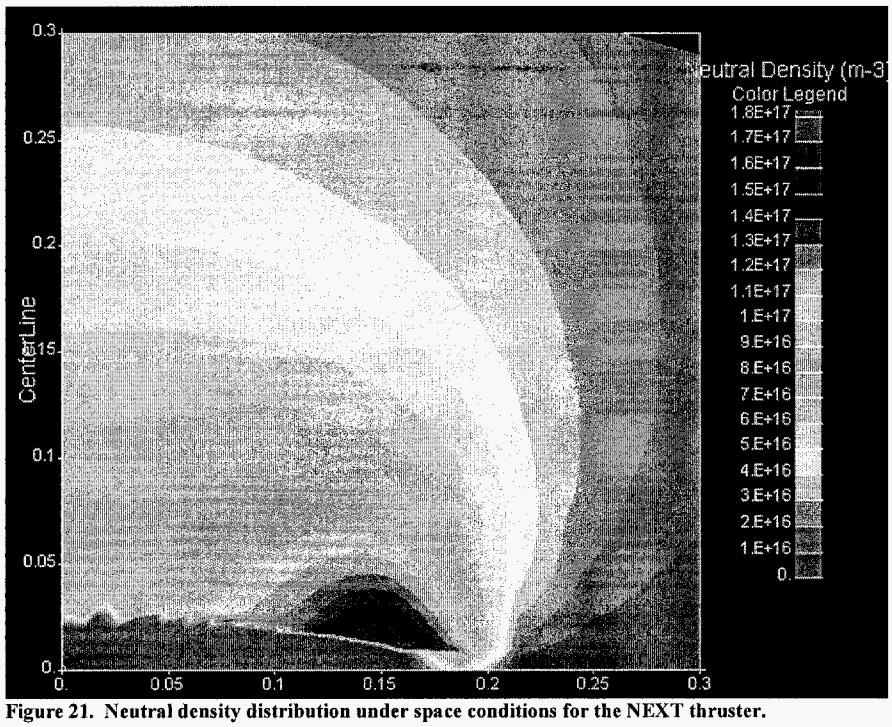

Figure 21. Neutral density distribution under space conditions for the NEXT thruster.

David Vaughan 5/2/05 1:58 PM
Deleted: 23

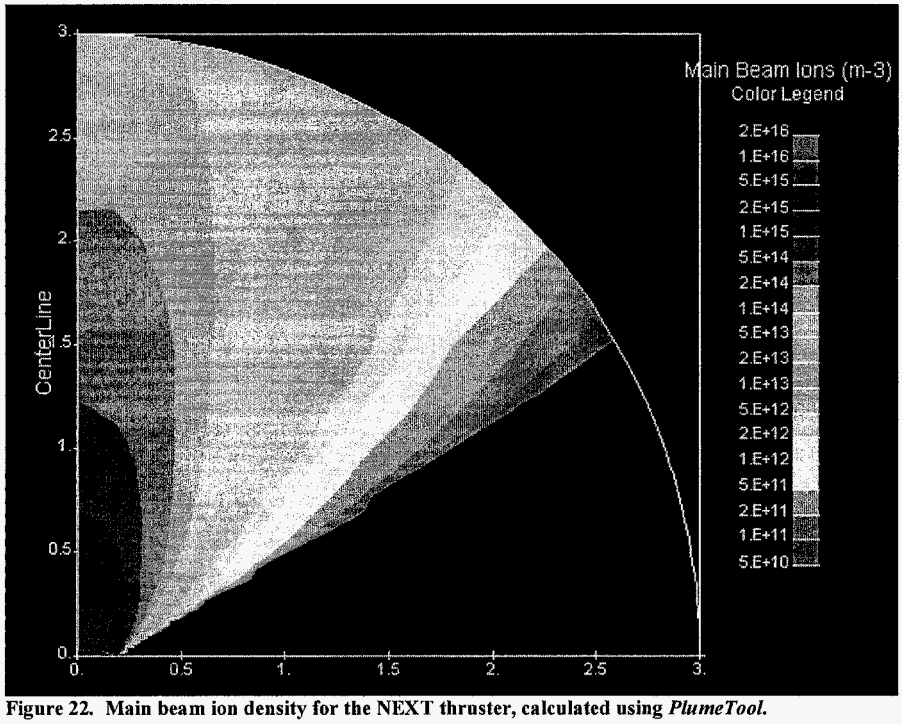

Figure 22. Main beam ion density for the NEXT thruster, calculated using *PlumeTool*.

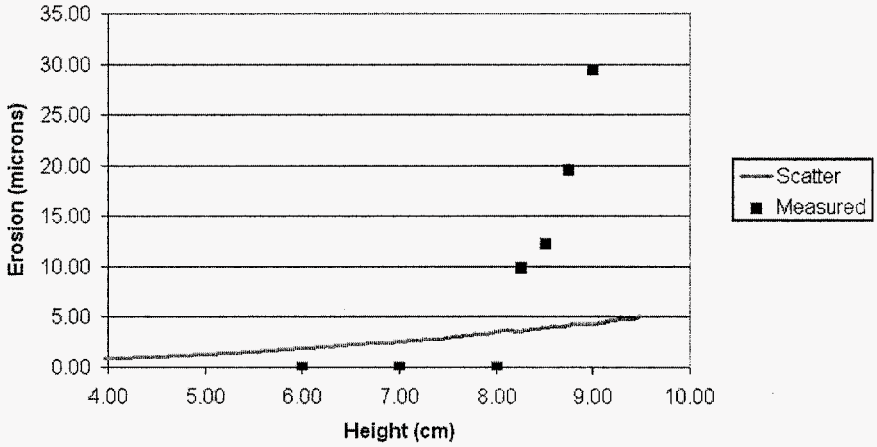

Figure 23. Neutralizer erosion (microns per 1000 hours) for the NEXT thruster. Calculation is for elastically scattered ions only, and data is from the 2000 hour wear test.

David Vaughan 5/2/05 1:58 PM
Deleted: 23

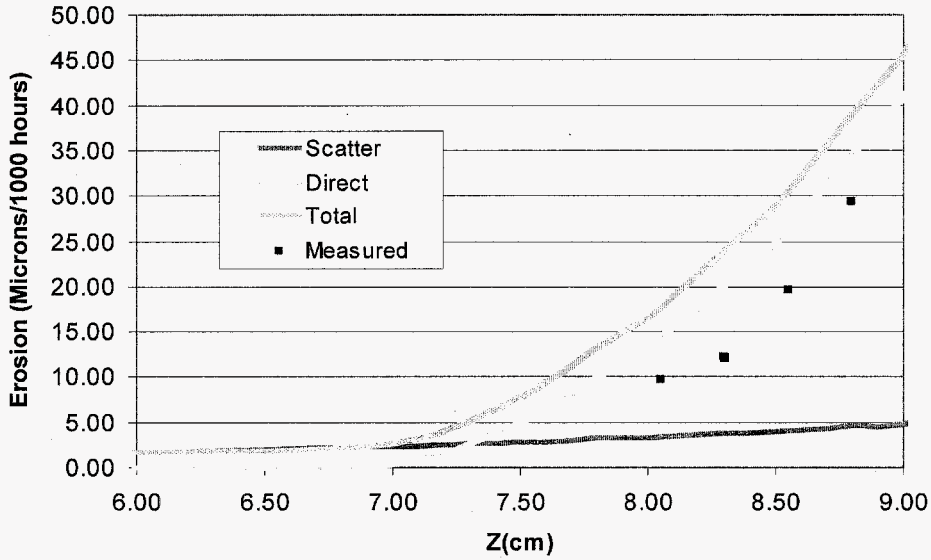

Figure 24. Calculation of erosion of the NEXT neutralizer, including direct impingement of primary ions, compared with measurement.

Conclusions

This paper details a methodology for calculating erosion of surfaces located at high angles (~45 degrees) to the beam direction of electrostatic ion thrusters. The methodology was applied to erosion of the neutralizer tube observed in long duration ground tests of the NEXT and NSTAR thrusters.

Two sources of energetic ions were considered. We first considered elastic scattering of beam ions by neutrals, which may come from the thruster or be part of the chamber background. We found that these ions were insufficient to cause the erosion observed on the top one to two centimeters of the neutralizer, although they may be responsible for erosion observed farther from the tip. We then considered direct impingement of primary ions on the neutralizer, which led to good agreement with the observed erosion. We further demonstrated that direct impingement of the neutralizer could be defeated by masking the outer two centimeters of the NEXT thruster's ion optics.

Key to adequate treatment of both the primary ions and elastically scattered ions was use of the *CEX2D* code to calculate the angular distribution of beamlet ions as a function of beamlet current. For both thrusters we found that low current beamlets contain ions out to angles in excess of 30 degrees, which, when added to approximately 15 degrees due to

David Vaughan 5/2/05 1:58 PM
Deleted: 23

dishing of the ion optics, leads to primary ions at about 45 degrees. The *PlumeTool* code proved to be an effective tool for calculating erosion due to elastically scattered ions.

We also noted that a large fraction of the erosion due to elastic scattering is due to the chamber background density. We performed calculations for space conditions by omitting this background density. The results are shown in Table 2. Erosion due to elastic scattering in space is a factor of two to three less than under laboratory conditions. Of course, this effect does not apply to direct impingement of primary beam ions.

Table 2. Erosion (microns per thousand hours) of the neutralizer tip due to elastically scattered ions under Lab and Space conditions.

	Lab	Space
NEXT Unmasked	4.8	1.6
NEXT Masked	3.3	1.4
NSTAR	1.0	0.4

In summary, we have performed calculations of the neutralizer erosion seen in ground tests of the NEXT and NSTAR thrusters. Both elastically scattered ions and high-angle primary beam ions contribute to the erosion, with the latter being dominant. We expect the erosion by elastically scattered ions to be considerably lower in space than under laboratory conditions.

---

[1] Sengupta, A., J. Brophy, J. Anderson, C. Garner, B. Banks, K. Groh, "An Overview of the Results from the 30,000 Hr Life Test of Deep Space 1 Flight Spare Ion Engine," AIAA Paper 2004-3608.
[2] Soulas, G. C., H. Kamhawi, M. J. Patterson, M. A. Britton, M. M. Frandina, "NEXT Ion Engine 2000 Hour Wear Test Results," AIAA Paper AIAA-2004-3791.
[3] Mikellides, I. G., Kuharski, R. A., Mandell, M. J., Gardner, B. M., "Assessment of Spacecraft Systems Integration Using The Electric Propulsion Interactions Code (*EPIC*)," AIAA-2002-3667, 2002.

[4] Brophy, J. R., I. Katz, J. E. Polk, J. R. Anderson, "Numerical Simulations of Ion Thruster Accelerator Grid Erosion," AIAA-2002-4261, 2002.

[5] Polk., J. E., J. R. Anderson, J. R. Brophy, V. K Rawlin, M. J. Patterson, J. Sovey, H. Harnley, "An Overview of Results from an 8200 Hour Wear Test of the NSTAR Ion Thruster," AIAA Paper 99-2446.
[6] Kamhawi, H., G. C. Soulas, M. J. Patterson, M. M. Frandina, "NEXT Ion Engine 2000 hour Wear Test Plume and Erosion Results," AIAA Paper 2004-3792.
[7] Clausing, P., "The Flow of Highly Rarefied Gases through Tubes of Arbitrary Length," *J. Vac. Sci. and Tech 8*, 636-646 (1931).

[8] Beijerinck, H. C. W., M. P. J. M. Stevens and N. F. Verster, "Monte-Carlo Calculation of Molecular Flow Through a Cylindrical Channel," *Physica 83C* 209-219 (1976).

David Vaughan 5/2/05 1:58 PM
Deleted: 23

[9] Sengupta A., D. Goebel, D. Fitzerald, Al Owens, G. Tynan, "Experimentally Determined Neutral Density and Plasma Parameters in a 30cm Ion Engine," AIAA Paper 2004-3613.

[10] Katz, I., *et al.*, "A Hall Effect Thruster Plume Model Including Large-Angle Elastic Scattering," AIAA Paper 01-3355, July 2001.

[11] Mikellides, I.G., Katz, I., Kuharski, R.A., and Mandell, M.J., "Elastic Scattering of Ions in Electrostatic Thruster Plumes," *Journal of Propulsion and Power 21*, 111-118 (2005).

[12] Yamamura, Y. and H. Tawara, "Energy Dependence of Ion-Induced Sputtering Yields From Monatomic Solids at Normal Incidence", *Atomic Data and Nuclear Data Tables, 62*, 149-253, (1996).
[13] Yamamura, Y., "An Empirical Formula for Angular Dependence of Sputtering Yields," *Radiation Effects 80*, 57-72 (1984).

David Vaughan 5/2/05 1:58 PM
Deleted: 23